Available online at www.sciencedirect.com

ScienceDirect

journal homepage: www.elsevier.com/locate/he

Stability of $LaNi_{5-x}Sn_x$ cycled in hydrogen

E.M. Borzone [a,b,*], M.V. Blanco [a,b], A. Baruj [b,c], G.O. Meyer [b,c]

[a] Agencia Nacional de Promoción Científica y Tecnológica, Argentina
[b] Centro Atómico Bariloche and Instituto Balseiro, Comisión Nacional de Energía Atómica, Argentina
[c] CONICET, Argentina

ARTICLE INFO

Article history:
Received 16 October 2013
Accepted 5 December 2013
Available online 6 January 2014

Keywords:
Hydride
AB5
Degradation
Purification
Structure

ABSTRACT

In this work we study the effect of cycling in hydrogen with a purity grade 4.5 of six alloys belonging to the $LaNi_{5-x}Sn_x$ family for $0 \leq x \leq 0.5$. Measurements consist in the alternate repetition of absorption reactions at a temperature of 316 K and an initial pressure of 800 kPa, each followed by a desorption reaction at the same temperature and a maximum backpressure of 2 kPa. All samples present good stability, preserving at least 98% of their initial capacity after 100 cycles. Samples with composition $LaNi_5$ and $LaNi_{4.55}Sn_{0.45}$ were subjected to 1000 cycles, after which we observe a higher stability from the Sn-containing alloy (96% of the initial capacity preserved versus 92% for $LaNi_5$). Absorption characteristic times do not suffer important changes in either case. Desorption is gradually retarded when Sn content is higher than 0.4 at.

1. Introduction

Applications based on the use of hydride forming materials usually require the repetition of hydrogen absorption/desorption cycles (ADC). During the absorption stage the material stores hydrogen by forming the hydride phase. During desorption, which is induced by lowering the external pressure or by increasing the temperature, the hydride decomposes and gaseous hydrogen is released. After several ADC, the materials may show a series of changes either morphological (particle size decrease), superficial (contamination with impurities that might be present in the gas) and/or structural (amorphization, disproportionation and appearance of stabler phases). These processes can lead to undesired changes in the overall material performance that could even prevent its use. It is then of vital importance to determine the behavior of hydrides under extended cycling in hydrogen.

Among candidates for stationary applications such as hydrogen separation and purification, compression, or in-house storage, $LaNi_{5-x}Sn_x$ alloys appear as good candidates due to their low reaction pressure at room temperature and fast reaction kinetics [1]. Existing data on the stability of these alloys are mostly related to their behavior under thermal cycling. For example, Lambert et al. [2] used a closed-loop device in order to perform up to 10000 thermal cycles between room temperature and 398 K on two alloys: $LaNi_{4.8}Sn_{0.2}$ and $LaNi_{4.27}Sn_{0.24}$. They found these materials to be highly resistant to thermal ADC, as their storage capacity decreased by 10% after 1500 cycles and by 15% after 10000 cycles. Bowman et al. found that a small addition of Sn improves the system resistance to extended thermal cycling [3].

Laurencelle et al. [1] and Araki et al. [4], on the other hand, studied pressure induced ADC on $LaNi_{4.8}Sn_{0.2}$. Both found a slight reduction in the storage capacity, of about 2%, after 1000 and 300 cycles, respectively. This is so far the only information

* *Corresponding author*. Centro Atómico Bariloche, Av. Bustillo 9500, 8400 Bariloche, Argentina. Tel.: +54 294 4445278; fax: +54 294 4445299.
E-mail addresses: emiliano.borzone@ib.edu.ar, manque.borzone@gmail.com (E.M. Borzone).
0360-3199/$ – see front matter
http://dx.doi.org/10.1016/j.ijhydene.2013.12.031

Table 1 – Alloy designation and chemical composition.

Alloy	La (at.)	Ni (at.)	Sn (at.)
Sn00	Bal.	5.00	0.00
Sn01	Bal.	4.82	0.18
Sn02	Bal.	4.73	0.27
Sn03	Bal.	4.66	0.34
Sn04	Bal.	4.55	0.45
Sn05	Bal.	4.49	0.51

available about pressure ADC in Sn substituted alloys. As part of a systematic effort to study the properties of $LaNi_{5-x}Sn_x$ alloys from an application oriented point of view, we have studied the pressure ADC behavior of these alloys for $0 \leq x \leq 0.5$. This is the complete composition range of interest for practical uses of these hydride forming materials.

2. Experimental details

The alloys were prepared by arc melting under Ar starting from the pure elements La (99.9%), Ni (99.95%) and Sn (99%). Alloys were re-melted several times in order to improve their homogeneity. The resulting buttons, of about 10 g each, were then heat treated at 1223 K for 48 h in individual quartz capsules containing Ar atmosphere. Chemical composition values were determined by atomic absorption spectroscopy (Table 1). For details on the sample preparation procedure and the resulting characteristics of the alloys, see Ref. [5].

ADC studies were performed on 1 g samples prepared from the alloy buttons. Samples were first activated by applying a hydrogen pressure of 60 bar and heating them to 345 K for 20 min. After this treatment, they were left to cool down to room temperature inside the reactor. Then, the reactor was evacuated by means of a rotary vane mechanical pump for 5 min to let the sample desorb, after which an extra absorption/desorption cycle was performed at room temperature by increasing/decreasing the hydrogen pressure. Cycling measurements were performed on the activated samples at a constant temperature of 316 K by means of an open-ended apparatus developed at our laboratory. The equipment works on the basis of a volumetric measurement method. Automatized solenoid valves allow hydrogen to enter/leave the reactor in repetitive cycles controlled by a personal computer and a home made program. Each pressure cycle is constituted of an absorption stage and a desorption stage. During the absorption stage, the initial hydrogen pressure is set by opening the inlet solenoid valve, which is connected in line with a needle valve that finely regulates the hydrogen flow into an intermediate chamber of about 80 cm^3. Once the desired pressure is achieved, the inlet valve is closed and the intermediate chamber is put in contact with the reactor of about 10 cm^3. In this manner, each cycle initiates at a fixed pressure of 800 kPa and composition values are calculated from the pressure drop. For desorption the free volume was 160 cm^3 and the backpressure was kept below 2 kPa by evacuating the vessel in a controlled manner when necessary. The gas used was 4.5° purity hydrogen.

Possible changes in structural parameters and phase stability were studied by means of X-ray powder diffraction (XRD). Samples were measured at room temperature using a PC controlled Philips PW3710 diffractometer in $\theta - 2\theta$ geometry with Cu K_α radiation at 40 kV. The receiving slit

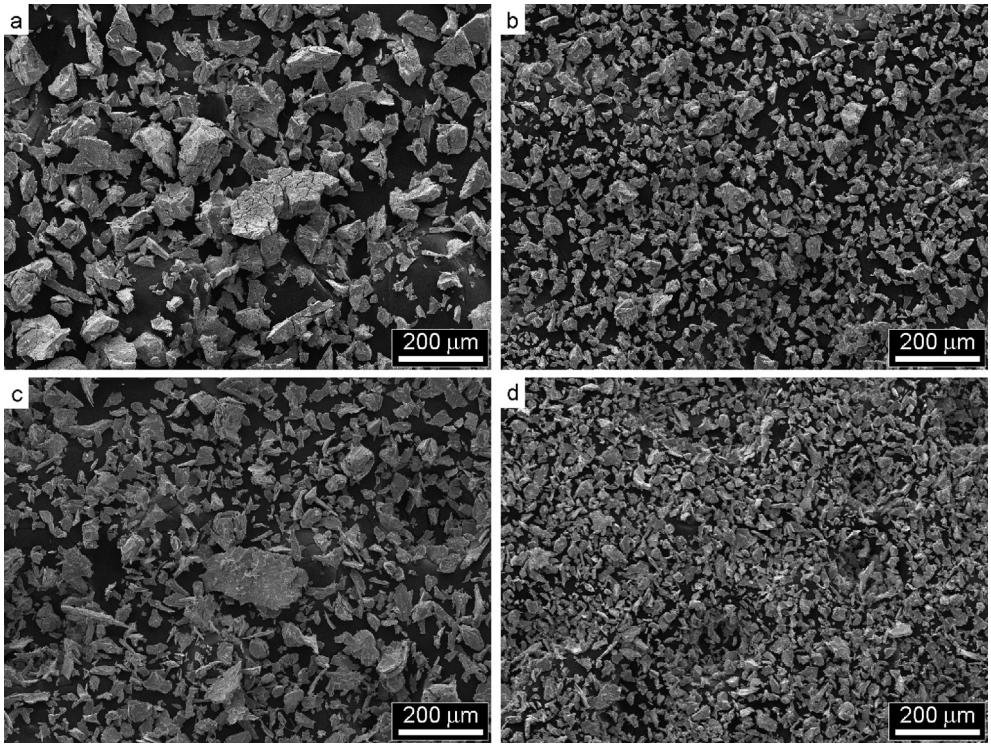

Fig. 1 – SEM images of $LaNi_5$ (a and b) and $LaNi_{4.55}Sn_{0.45}$ (c and d) after 3 cycles (a and c) and after 1000 cycles (b and d). ADC results in decrepitation.

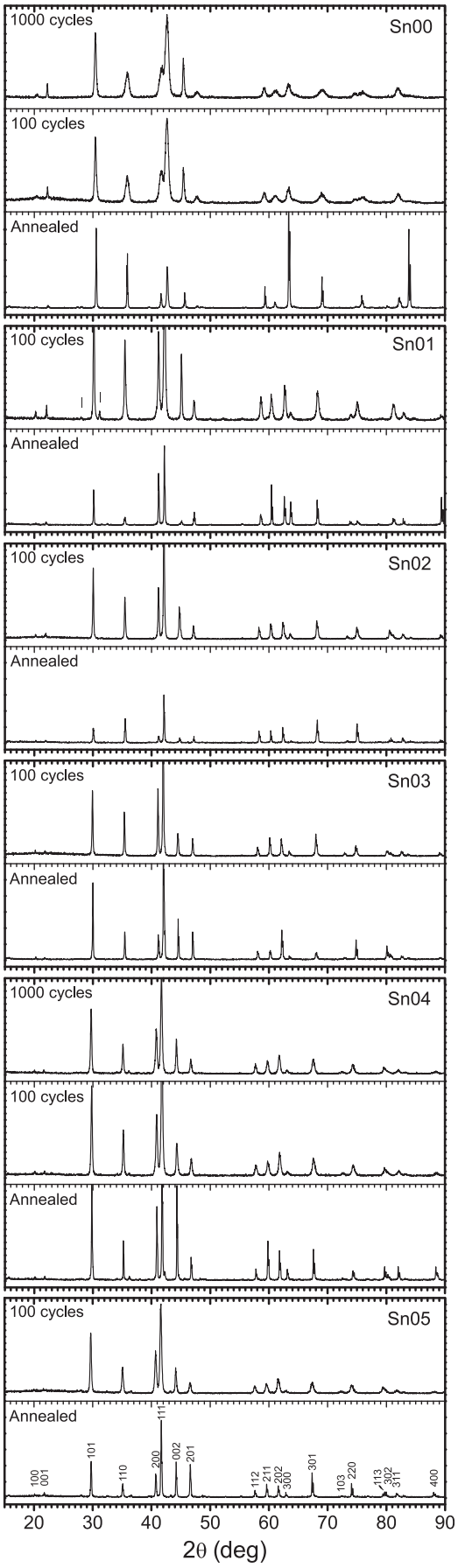

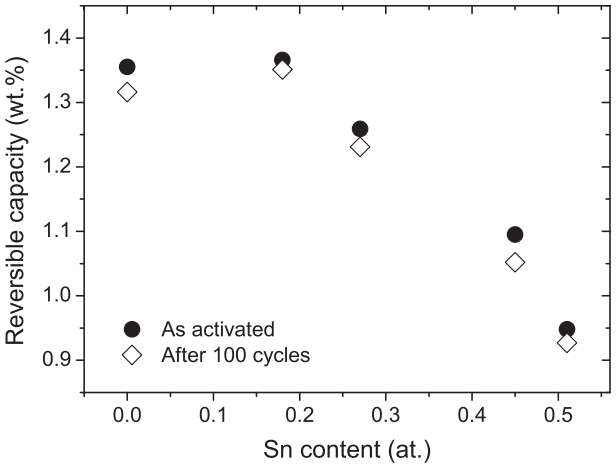

Fig. 3 – Effect of 100 pressure cycles on the reversible hydrogen absorption capacity of $LaNi_{5-x}Sn_x$ alloys.

size was 0.1 mm, the step was 0.02° and the exposition time was 1 s by step. The scanned 2θ angles ranged from 10° to 90°. Changes in the powder morphology before and after ADC were observed with secondary electrons in a Philips 515 scanning electron microscope (SEM) operating at 30 kV.

3. Results and discussion

3.1. *Decrepitation*

The as-activated $LaNi_5$ has a typical particle size of about 40 μm, with most of the material distributed in particles of 10 μm–200 μm (Fig. 1a). After 1000 ADC the typical size is reduced to about 10 μm, with a distribution between 5 μm and 50 μm (Fig. 1b). For Sn-containing samples a lower amount of mid- to bigger sized particles (>40 μm) is found on the activated material (Fig. 1c), suggesting that decrepitation occurs faster than for $LaNi_5$. In all cases the bigger particles are heavily fractured and they could be considered as composed by a group of smaller particles. The effect of 1000 ADC on powder morphology can be observed in Fig. 1d. The material decrepitates and final particle size is similar to that of $LaNi_5$ with a smaller proportion of bigger particles. Decrepitation of AB_5 alloys after ADC is a well established phenomenon. It arises from the large difference between the cell volume of the metallic and hydride phases, of about 21% [6]. This volume difference cannot be accommodated by means of the elastic distortion of the matrix and it generates tensions, crystalline defects and fractures during the reaction, pulverizing the material.

Fig. 2 – XRD results for the complete set of alloys under study. In each case, the results for the annealed material and after 100 ADC are presented. In the case of Sn01 after 100 ADC, a small amount of LaH_2 is detected (marked in the corresponding figure). In addition, XRD measurements of samples Sn00 and Sn04 after 1000 ADC are included.

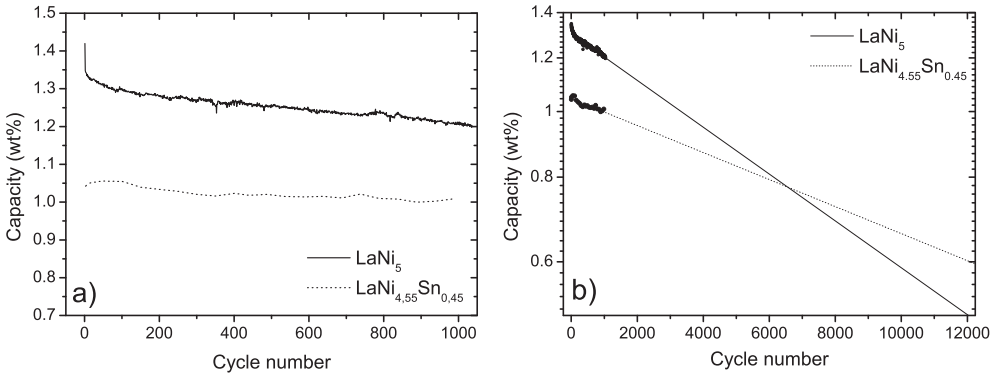

Fig. 4 – a) Extended cycling degradation of the reversible hydrogen capacity of $LaNi_5$ (Sn00) and $LaNi_{4.55}Sn_{0.45}$ (Sn04) alloys. Sn addition reduces initial capacity and decreases the rate of degradation. b) Exponential extrapolation of data shown in (a). Both alloys would present the same capacity after about 6500 cycles.

3.2. *Structure*

XRD measurements of the annealed alloys before interacting with hydrogen show a single P6/mmm phase, in accordance with previous reports [7]. Lattice parameters increase as the Sn content of the alloy increases [8]. Compared to the annealed state, after 100 ADC no new phases were detected for all alloys but Sn01 (Fig. 2). In the case of alloy Sn01, a small amount of LaH_2 formed after cycling (Fig. 2). For alloys Sn00 and Sn04 XRD measurements were also taken after 1000 ADC. The results closely resemble those obtained after 100 ADC where, again, no new phases appeared. In this sense, possible disproportionation products for AB_5 alloys [9] such as metallic Ni or Lanthanum hydrides were generally not observed after cycling within the detection limit of the XRD equipment with the mentioned exception of alloy Sn01 where the detected amount of LaH_2 is small.

Cell parameters calculated from the XRD patterns do not show significant changes after 100 cycles for any of the studied materials. The main difference that can be observed for this set of XRD measurements is a significant line broadening for the Sn00 ($LaNi_5$) alloy after ADC, which is not observed in any of the other cases. Considering that the final particle size obtained after decrepitation is similar for all these materials, this line broadening could be related to the formation of a higher defect density in Sn00 with ADC.

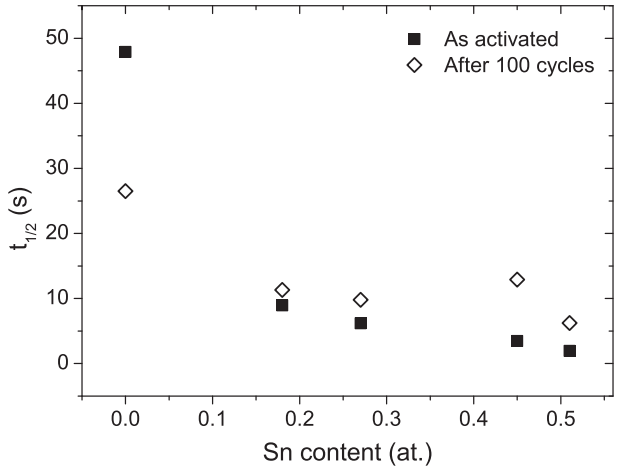

Fig. 5 – Dependence of the hydrogen absorption characteristic time ($t_{1/2}$) with the Sn content for as-activated and cycled (100 ADC) samples.

3.3. *Hydrogen reversible capacity*

The observed hydrogen reversible capacity for all alloys presented good cycling stability. In all cases, about 98% of the hydrogen reversible capacity was preserved after 100 cycles. Differences found among different samples between the as-activated state and after 100 cycles lay within the experimental uncertainties (Fig. 3), although in all cases a slightly lower capacity was measured after ADC. In particular, the capacity of the $LaNi_{4.8}Sn_{0.2}$ alloy (Sn01) after 100 cycles is higher than that of $LaNi_5$, in accordance with previous results from Araki and collaborators [4].

In order to discern the effect of Sn on the cycling life of these materials, extended cycling was performed for alloys Sn00 and Sn04. After 1000 cycles $LaNi_{4.55}Sn_{0.45}$ (Sn04) has lost about 4% of its initial reversible hydrogen capacity, thus showing a better stability than $LaNi_5$ (Sn00), which presents an 8% loss (Fig. 4a). $LaNi_5$ has a higher initial hydrogen capacity than $LaNi_{4.55}Sn_{0.45}$. This advantage from the point of view of storage capacity would eventually disappear as ADC proceeds, as it was observed for alloy Sn01 after 100 cycles. In order to obtain a rough estimate of the behavior under more extended cycling, the data were extrapolated by means of an exponential curve, following the procedure used in Refs. [10–12]. Using this approach the mean cycle life, defined as the number of cycles at which the alloy losses 50% of its initial hydrogen storage capacity, would be of about 8200 cycles for $LaNi_5$ and 16000 cycles for $LaNi_{4.55}Sn_{0.45}$. According to this estimate, both alloys would present the same capacity after about 6500 cycles (Fig. 4b).

The reason for the improved cycling resistance of Sn containing alloys in comparison to $LaNi_5$ is not completely clear. Two mechanisms have been proposed as responsible for the cycling degradation observed in AB_5 alloys. The first proposed mechanism, disproportionation, is linked to the gradual formation of stable LaH_x hydrides and segregation of metallic Ni as cycling proceeds [9]. Based on TEM observations of thermally cycled alloys $LaNi_{4.9}Sn_{0.1}$ and $LaNi_{4.8}Sn_{0.2}$, Bowman et al.

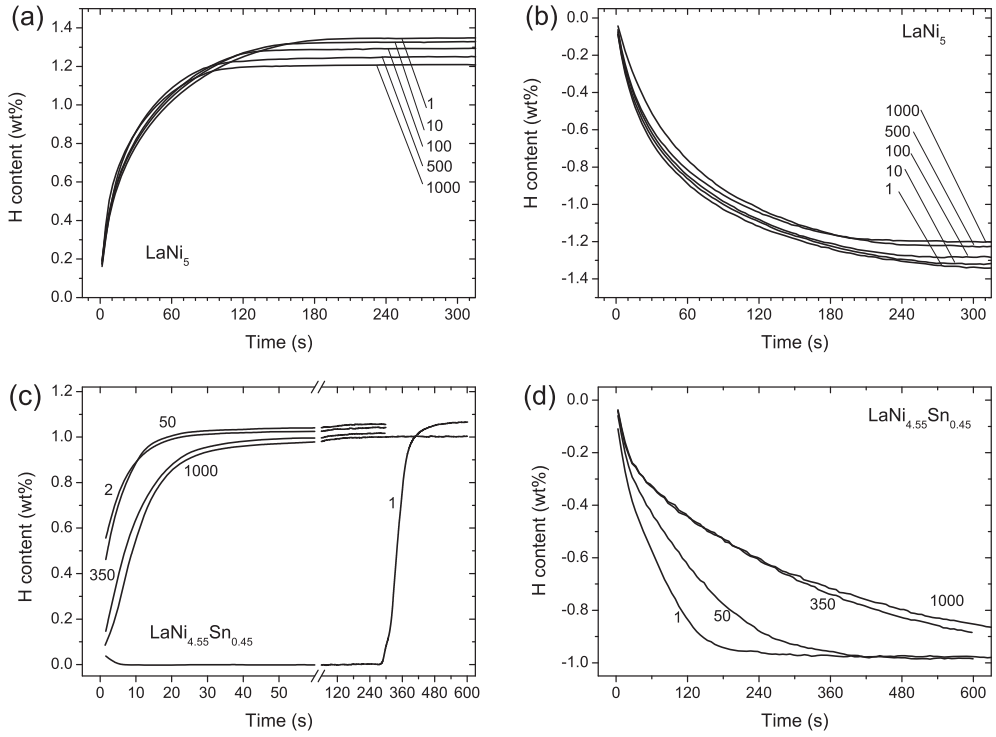

Fig. 6 – Hydrogen reaction as a function of time for: $LaNi_5$: a) absorption, b) desorption; and $LaNi_{4.55}Sn_{0.45}$: c) absorption, d) desorption. The cycle number is indicated close to each curve.

proposed that Sn addition affects the disproportionation kinetics effectively retarding the formation of stable hydrides [3]. We have not detected the formation of significant amounts of additional phases after 100 and 1000 cycles (Fig. 2), indicating that disproportionation would be a minor factor up to that cycle range. Also in accordance, Laurencelle et al. reported that no additional phases were found in XRD measurements of $LaNi_{4.8}Sn_{0.2}$ after 1000 cycles [1]. The second proposed degradation mechanism is related to the possibility of irreversibly trapping hydrogen in lattice defects such as vacancies and dislocations [13]. Initially, Nakamura et al. proposed that Sn inhibited the formation of dislocations in the material [13]. Although Matsuda et al. [14] observed the formation of a-type dislocations in $LaNi_{4.75}Sn_{0.25}$ after 5 ADC, the results from positron measurements reported by Araki et al. confirm that Sn retards the formation of trapping defects [4]. The larger line broadening observed for $LaNi_5$ in comparison with the rest of Sn containing alloys observed in the present experiments (Fig. 2), could indicate that, indeed, cycling results in a higher density of defects in the Sn-free material and a faster degradation of its reversible capacity. Both mechanisms could be related with a more homogeneous distribution of hydrogen within the Sn-containing alloys with respect to $LaNi_5$, as it was observed by Fultz et al. [15]. They suggested that this effect could diminish the internal stresses that cause defect formation, which could in turn explain the smaller vacancy and dislocation density observed by Nakamura and Araki, and the marked line broadening reported here for $LaNi_5$. At the same time, a reduced reversible defect formation density during the reaction would diminish the migration of metal atoms, potentially retarding the formation of Ni clusters and LaH_x precipitates.

3.4. *Reaction kinetics*

Along the cycling experiments the materials suffer modifications that can alter their reaction kinetics. On one hand, particle size decreases, shortening diffusion paths and increasing the exposed surface in contact with the gas (Fig. 1). Additionally, defects are generated, that could increase the diffusivity of atomic H within the material [14]. On the other hand, the surface may lose reactivity due to the accumulation of impurities present in the gas [16,17]. These effects compete to define the reaction kinetics characteristics as cycling proceeds. Hydrogen sorption kinetics can be analyzed in terms of a characteristic time ($t_{1/2}$), defined as the time taken to reach half the total capacity. Under the conditions used for this study, the initial absorption kinetics increased as the Sn content in the alloy increases [5]. After 100 cycles this tendency persists, but is less marked (Fig. 5).

For extended cycling experiments (1000 cycles), the $LaNi_5$ initial reaction rate is maintained (Fig. 6a). However, as the final capacity is lower, the characteristic time $t_{1/2}$ is also lower. Desorption kinetics is slightly retarded by cycling (Fig. 6b).

In the case of alloys containing Sn, we found a similar behavior to that of $LaNi_5$ for alloys Sn01, Sn02 and Sn03. The effect of cycling on the reaction kinetics of these low-Sn alloys has been already reported by Laurencelle et al. [1]. Considering an alloy containing a higher Sn content, $LaNi_{4.55}Sn_{0.45}$, the absorption kinetics is essentially not affected by cycling (Fig. 6c). Changes in the hydrogen absorption rate are minor, consistent with a small retardation. In comparison, gradual retardation is important for desorption kinetics (Fig. 6d). This effect could in part be related to the low desorption pressures of these higher-Sn content alloys, which result in a lower driving force for desorption [5].

4. Conclusions

The studied materials presented significant morphological changes after cycling in hydrogen, being pulverized up to mean typical sizes of about 10 μm. Structure was preserved after 100 cycles and 1000 cycles. Cell parameters did not show important changes. Significant amounts of new phases were not detected by means of XRD.

All studied alloys presented an adequate resistance to hydrogen absorption–desorption cycling. Partial substitution of Ni by Sn improves the alloy stability. However, as the original $LaNi_5$ material is itself very stable, this difference only becomes apparent after several thousand cycles. Capacity loss is not due to disproportionation as this has not been detected by XRD.

Absorption kinetics is relatively stable. Under the studied conditions, $LaNi_5$ kinetics improves by cycling while Sn-containing alloys kinetics are slightly retarded. Desorption kinetics is retarded for all alloys, more importantly for the ones with higher Sn additions (>0.4 at.).

Based on these results, $LaNi_{5-x}Sn_x$ alloys are found to be potentially useful for their use in hydrogen capture devices.

Acknowledgments

The authors acknowledge the help of S. Rivas, F. Roldán, E. Aburto and M. Isla for their help in the preparation of samples. C. Osuna helped with alloys chemical analysis. This work has been supported by ANPCyT (PAE 36985 and PICT 2012-1796) and by ANPCyT-CNEA through fellowships from PFDT-PRH 200.

REFERENCES

[1] Laurencelle F, Dehouche Z, Goyette J. Hydrogen sorption cycling performance of $LaNi_{4.8}Sn_{0.2}$. J Alloys Compd 2006;424:266–71.

[2] Lambert SW, Chandra D, Cathey WN, Lynch FE, Bowman RC. Investigation of hydriding properties of $LaNi_{4.8}Sn_{0.2}$, $LaNi_{4.27}Sn_{0.24}$ and $La_{0.9}Gd_{0.1}Ni_5$ after thermal cycling and aging. J Alloys Compd 1992;187:113–35.

[3] Bowman Jr RC, Luo CH, Ahn CC, Witham CK, Fultz B. The effect of tin on the degradation of $LaNi_{5-y}Sn_y$ metal hydrides during thermal cycling. J Alloys Compd 1995;217:185–92.

[4] Araki H, Date R, Sakaki K, Mizuno M, Shirai Y. Positron lifetime study on the degradation of $LaNi_5$ and $LaNi_{4.8}Sn_{0.2}$ during hydrogen absorption-desorption cycling. Phys Stat Sol (c) 2007;4(10):3510–3.

[5] Borzone EM, Baruj A, Blanco MV, Meyer GO. Dynamic measurements of hydrogen reaction with $LaNi_{5-x}Sn_x$ alloys. Int J Hydrogen Energy 2013;38:7335–43.

[6] Stange M, Maehlen JP, Yartys VA, Norby P, van Beek W, Emerich H. In situ SR-XRD studies of hydrogen absorption–desorption in $LaNi_{4.7}Sn_{0.3}$. J Alloys Compd 2005;404–406:604–8.

[7] Cantrell JS, Beiter TA, Bowman Jr RC. Crystal structure and hydriding behavior of $LaNi_{5-y}Sn_y$. J Alloys Compd 1994;207–208:372–6.

[8] Luo S, Clewley JD, Flanagan TB, Bowman Jr RC, Wade LA. Further studies of the isotherms of $LaNi_{5-x}Sn_x - H$ for $x = 0–0.5$. J Alloys Compd 1998;267:171–81.

[9] Goodell PD. Stability of rechargeable hydriding alloys during extended cycling. J Less-Common Met 1984;99:1–14.

[10] Nishimura K, Sato K, Nakamura Y, Inazumi C, Oguro K, Uehara I, et al. Stability of $LaNi_{5-x}Al_x$ alloys ($x = 0 \sim 0.5$ during hydriding and dehydriding cycling in hydrogen containing O_2 and H_2O. J Alloys Compd 1998;268:207–10.

[11] Mordkovich VZ, Korostyshevsky NN, Baychtok YuK, Mazus EI, Dudakova NV, Mordovin VP. Degradation of $LaNi_5$ by thermobaric cycling in hydrogen and hydrogen–nitrogen mixture. Int J Hydrogen Energy 1990;15:723–6.

[12] Sandrock GD, Goodell PD. Cyclic life of metal hydrides with impure hydrogen: overview and engineering considerations. J Less-Common Met 1984;104:159–73.

[13] Nakamura H, Nakamura Y, Fujitani S, Yonezu I. Cycle performance of a hydrogen-absorbing $La_{0.8}Y_{0.2}Ni_{4.8}Mn_{0.2}$ alloy. Int J Hydrogen Energy 1996;21:457–60.

[14] Matsuda J, Nakamura Y, Akiba E. Lattice defects introduced into $LaNi_5$-based alloys during hydrogen absorption/desorption cycling. J Alloys Compd 2011;509:7498–503.

[15] Fultz B, Witham CK, Udovic TJ. Distributions of hydrogen and strains in $LaNi_5$ and $LaNi_{4.75}Sn_{0.25}$. J Alloys Compd 2002;335:165–75.

[16] Uchida H, Seki S, Seta S. Effect of surface contamination on the hydriding behaviors of $LaNi_{4.5}Al_{0.5}$, $LaNi_{2.5}Co_{2.5}$ and $LaNi_{4.5}Mn_{0.5}$. J Alloys Compd 1995;231:403–10.

[17] Sato M, Uchida H, Stange M, Yartys VA, Kato S, Ishibashi Y, et al. H_2 reactivity on the surface of $LaNi_{4.7}Sn_{0.3}$. J Alloys Compd 2005;402:219–23.